Cathodoluminescence Investigation of Residual Stress in Er 3+ :YAlO 3 Thin Films Grown on (110) SrTiO 3 Substrate by Metal−Organic Chemical Vapor Deposition

ARTICLE *in* THE JOURNAL OF PHYSICAL CHEMISTRY B · DECEMBER 2006

Impact Factor: 3.3 · DOI: 10.1021/jp064396y · Source: PubMed

6 AUTHORS, INCLUDING:

Roberta G. Toro
National Research Council
62 PUBLICATIONS **620** CITATIONS
SEE PROFILE

Graziella Malandrino
University of Catania
172 PUBLICATIONS **2,137** CITATIONS
SEE PROFILE

Ignazio L Fragalà
University of Catania
320 PUBLICATIONS **6,332** CITATIONS
SEE PROFILE

Keshu Wan
Southeast University (China)
31 PUBLICATIONS **294** CITATIONS
SEE PROFILE

Cathodoluminescence Investigation of Residual Stress in Er^{3+}:$YAlO_3$ Thin Films Grown on (110) $SrTiO_3$ Substrate by Metal-Organic Chemical Vapor Deposition

Roberta G. Toro,[†] Graziella Malandrino,[†] Ignazio L. Fragalà,*[,†] Wan Keshu,[‡] Andrea Leto,[‡] and Giuseppe Pezzotti*[,‡]

Dipartimento di Scienze Chimiche, Università di Catania, & INSTM, UdR Catania, Viale A. Doria 6, I-95125 Catania, Italy, and Ceramic Physics Laboratory & Research Institute for Nanoscience, RIN, Kyoto Institute of Tecnology, Sakyo-ku, Matsugasaki, 606-8585 Kyoto, Japan

Received: July 12, 2006; In Final Form: September 14, 2006

$YAlO_3$ thin films doped with different amounts of Er^{3+} have been grown directly onto (110) $SrTiO_3$ substrate using the metal-organic chemical vapor deposition method (MOCVD). X-ray diffraction patterns and the rocking curve of the (002) reflection point to the growth of ⟨001⟩-oriented $YAlO_3$ phase. Piezo-spectroscopic (PS) biaxial calibration was performed on two luminescence bands, related to transitions from the $^4S_{3/2}$ excited state, using a specially designed ball-on-ring loading jig. Such a PS calibration allowed us to retrieve the rate of wavelength shift with stress without separating the grown film from the substrate. The outcome of the PS calibration has been applied to build up in the field emission scanning electron microscope (FEG-SEM) high-resolution maps of the residual stress field developed in the film. Results indicate that the residual stress in Er^{3+}:$YAlO_3$ films were compressive in nature and increased with increasing Er^{3+} dopant concentration.

Introduction

Trivalent rare earth ions, introduced as substitutional elements in amorphous or crystalline matrixes,[1−5] are very attractive optical activators since they can emit in the ultraviolet, visible, and infrared wavelength range depending on excitation energy, dopant concentration, and structural properties of the host matrix. In this context, $YAlO_3$ can be considered to be an interesting host matrix for the realization of optical devices because of its high refractive index and thermal stability.[6] Recently, epitaxially grown $YAlO_3$ thin films doped with Er^{3+} in different concentrations have attracted much attention because of their potential use as planar wavelength laser with light propagation parallel to the plane of the substrate with the film acting as waveguide.[7,8]

Therefore, a high throughput technique, that may represent a potentially scalable process, is required for the fabrication of these films. In this context, metal-organic chemical vapor deposition (MOCVD)[9] represents a strategic challenge for these applications because of large deposition areas, conformal step coverage, lower deposition temperatures, and adaptability to large-scale processing.

To our knowledge, only one study has been reported up to date on the fabrication of YAP films by MOCVD.[10] Recently, we have achieved[11] a reproducible MOCVD procedure for the epitaxial synthesis of $YAlO_3$ thin films onto $SrTiO_3$ substrates. Structural, microstructural, and optical properties of these films have been already studied. However, in the perspective of technological applications as actual optical devices, it becomes of interest to precisely characterize the residual stress fields developed during the deposition process. It is known that residual stresses can lead to generation of microcracks, detachment of the film from the substrate, bending, and loss of optical efficiency. The residual stress field becomes of particular importance in thin film materials where it may become several orders of magnitude higher than in bulk materials.[12] The presence of residual stress of high magnitude in thin films has been reported to significantly affect mechanical, electrical, and optical properties, thus affecting the lifetime and the reliability of the devices.[13,14] In this context, an analytical technique with the capability of quantitatively visualizing residual stress distributions on the nanometer scale represents an important prerequisite for optimizing microstructure/property relationships.

The residual stress field in MOCVD thin films mainly consists of two components:[15,16] (1) one component that is related to the thermal field, namely, to the difference in the thermal expansion coefficients of the deposited film and the substrate, and (2) another component is the so-called intrinsic stress, which is the result of the conditions and method adopted for film growth. This latter component can be in a large part associated with the film microstructure and with the presence of impurities or dopants. The nature of the overall stress field, given by the superposition of the two above components, may be compressive or tensile, depending on film and substrate materials or on processing conditions.

Several techniques such as Raman scattering,[17−21] optical fluorescence,[22−24] X-ray diffraction,[25] laser reflectance,[26] cantilever beam deflection,[27,28] and wafer curvature measurements[29] have been used to determine residual stresses in thin films. In addition to these techniques, cathodoluminescence (CL) piezospectroscopy (PS) has been qualitatively used to measure residual stresses.[30] CL is the light emission produced as a result of the interaction between the material and an electron beam, and it is suitably applied concurrently to surface examination in the SEM. Recently, Pezzotti and co-workers[31−33] have shown that CL can represent a useful technique for quantitative stress assessments on a nanometer scale by using a field emission electron gun (FEG) SEM. These authors have applied a full CL spectroscopic analysis to measure nanoscale residual stresses

* Authors to whom correspondence should be addressed. E-mail: lfragala@dipchi.unict.it (I.F.); pezzotti@chem.kit.ac.jp (G.P.).
[†] Università di Catania.
[‡] Kyoto Institute of Tecnology.

10.1021/jp064396y CCC: $33.50
Published on Web 10/18/2006

in both amorphous and crystalline solids. This approach may take advantage of the intrinsic luminescence properties of semiconductor materials or of suitable rare-earth ions acting as "atomic-scale stress sensors" into the investigated material.

In this paper, we demonstrate that the CLPS technique can be used for the quantitative evaluation of the residual stresses stored in Er^{3+} doped $YAlO_3$ thin films epitaxially grown by MOCVD process on $SrTiO_3$ (110) substrates.

Experimental and Computational Procedures

Second-generation metal-organic complex precursors $Y(hfa)_3$·diglyme and $Er(hfa)_3$·monoglyme (Hhfa = 1,1,1,5,5,5-hexafluoro-2,4-pentanedione, monoglyme = dimethoxyethane, diglyme = bis(2-methoxyethyl)ether) were prepared as reported elsewhere[34] and were used without any further purification. $Al(acac)_3$ (Hacac = acetylacetone; purchased from Aldrich, Co.) was purified by sublimation. $YAlO_3$ thin films doped with 2 or 10 mol % Er^{3+} were grown in a horizontal hot-wall, low-pressure MOCVD reactor equipped with a single sublimation zone maintained at a temperature of 130 °C. Depositions were carried out for 45 min in the reactor chamber under 4 Torr. Deposition temperature was kept constant at 1050 °C. A typical growth rate of about 10 nm/min has been observed. Fluorine contamination was avoided through in-situ hydrolysis by introducing water vapor into the oxygen stream.[35] The ⟨110⟩-oriented $SrTiO_3$ substrates used in this investigation were commercially available wafers (produced by Crystal GmbH).

$\theta-2\theta$ X-ray diffraction (XRD) patterns and rocking curve measurements were recorded on a Bruker-AXS D5005 $\theta-\theta$ X-ray diffractometer, using Cu Kα radiation operating at 40 kV and 30 mA.

The FEG-SEM employed in this study was a new thermal filament type device with a lateral spatial resolution of 1.5 nm (JSM-6500F, JEOL, Tokyo, Japan). It was used for both morphological investigations and stress evaluations. The microscope was mounted within a cut-out on an air-suspended optical table to preclude vibration and to favor optical alignment. A high-sensitivity cathodoluminescence detector unit (MP-32FE, Horiba Ltd., Kyoto, Japan) was employed for the collection of light upon reflection into an ellipsoidal mirror and transmission through an optical fiber. The emitted CL spectrum was analyzed using a monochromator equipped with a CCD camera. A new mapping device (PMT R943-02 Select, Horiba Ltd., Kyoto, Japan) was used and related software was developed to enable collection with nanometer-scale spatial resolution and to automatically analyze large numbers of CL spectra in nearly real time. The signal from a neon discharge lamp was systematically collected, concurrently to each spectral measurement, to obtain an external wavelength reference. The collected spectra were analyzed using curve-fitting algorithms included in the LabSpec software package (Yobin Yvon Horiba) to determine the peak wavelength. A good quality luminescence spectrum of the luminescent Er^{3+} ion, suitable for precise mathematical fitting, could be collected within a few seconds of accumulation time. Spectral wavelength shifts were obtained from the difference between the spectral locations of the peak maximum under stressed (residual or externally applied stress) and unstressed conditions. The stress-free wavelength λ_0 was estimated by averaging about 5×10^5 spectra randomly collected on a detached and pulverized portion of each film. Calibrations of spectral shift versus externally applied stress were performed using a laboratory made ball-on-ring loading jig connected with a load cell to measure in situ the applied load.[36] At the center of the sample tensile surface loaded in the ball-on-ring biaxial bending jig, an equibiaxial stress magnitude (maximum radial stress, σ_r, equal to maximum tangential stress, σ_t) can be related to the applied load as follows:[37]

$$\sigma_{bi} = \sigma_r = \sigma_t = \sigma_{max} = \frac{3P(1+\nu)}{4\pi t^2}\left(1 + 2\ln\frac{D}{d} + \frac{1-\nu}{1+\nu}\frac{2D^2 - d^2}{4R^2}\right) \quad (1)$$

where P is the applied load, t is the plate thickness, D is the diameter of the ring, d is the diameter of the region of uniform stress at the plate center, R is half-planar dimension of the plate sample, and ν is the Poisson's ratio of the sample. The extent of the constant stress region at the center of the sample can be calculated from the Hertz elastic contact stress equation:[38]

$$d = d_{contact} = \left(\frac{3Pd_{ball}}{4\chi}\right)^{1/3} \quad (2)$$

$$\chi = \left(\frac{1-\nu_1^2}{E_1} + \frac{1-\nu_2^2}{E_2}\right)^{-1} \quad (3)$$

where d_{ball} is the diameter of the loading ball (=1.0 mm), and ν and E are the Poisson's ratio and the Young's modulus, respectively, of sample and loading ball (subscripts 1 and 2, respectively). For the stainless steel jig, $E_2 = 200$ GPa and $\nu_2 = 0.3$, while $E_1 = 225$ GPa and $\nu_1 = 0.28$ were taken for the (110) $SrTiO_3$ substrate. An assessment of the reliability of the present jig has been given in previously published papers.[36] The sample, mounted in correspondence of the center of the supporting ring, experienced a fixed load of 20 N and the spectral shift (averaged over about 10^3 points for each load) recorded along an arbitrary line scan. A strong bonding was assumed between the thin film and the substrate and, accordingly, the stress fields in Er^{3+}:$YAlO_3$ layer and in (110) $SrTiO_3$ substrate were simply related by the following equation:

$$\sigma_{YAlO_3} = \frac{Y_{YALO_3}}{Y_{SrTiO_3}}\sigma_{SrTiO_3} \quad (4)$$

where Y is the biaxial modulus of the material. The median value of the biaxial modulus of Er^{3+}:$YAlO_3$ and (110) $SrTiO_3$ was taken as 340 and 244 GPa, respectively. Finally, a biaxial PS coefficient, Π_{bi}, was obtained from a plot of the observed spectral shifts, $\Delta\lambda$, as a function of biaxial stress collected along a line scan direction.

The residual stress field stored in a thin film, which is biaxial in nature ($\sigma_R = \sigma_{xx} = \sigma_{yy}$ and $\sigma_{zz} = 0$, where x and y are in-plane axes, and z is normal to the film surface), can be related to the spectral shift, $\Delta\lambda$, by a linear equation:[39]

$$\Delta\lambda = \Pi_{bi}\sigma_R \quad (5)$$

this PS relationship remains linear up to magnitudes of several GPa.

Results and Discussion

Er^{3+}:$YAlO_3$ films showed mirrorlike surfaces after MOCVD growth. Scanning electron microscopy images showed that the films possess smooth surfaces and a uniform grain size distribution (Figure 1a and b for Er^{3+} concentration of 2 and 10 mol %, respectively). Moreover, SEM investigation shows

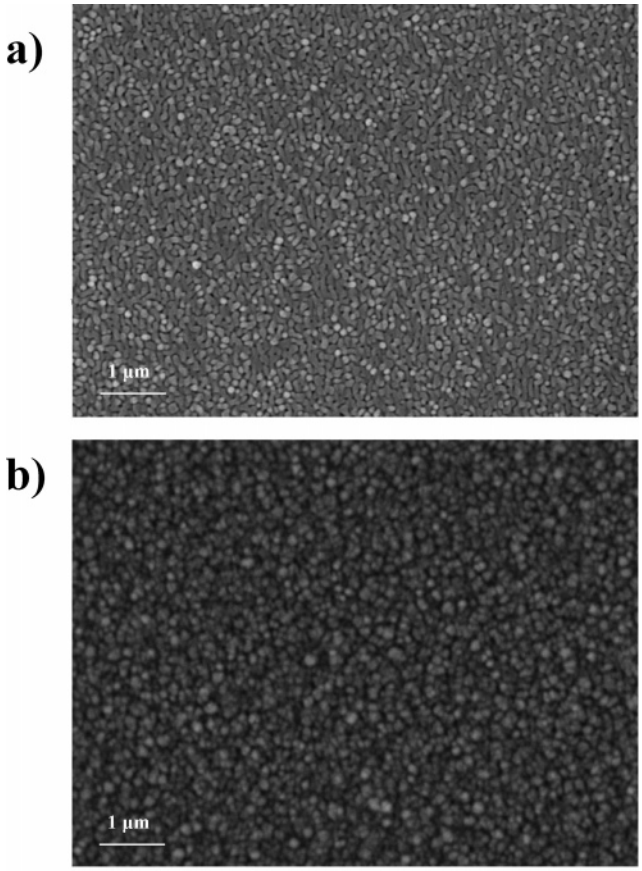

Figure 1. FEG-SEM images of the surface morphology of 2 mol % (a) and 10 mol % (b) Er^{3+} doped $YAlO_3$ thin films deposited on $SrTiO_3$ (110) substrate.

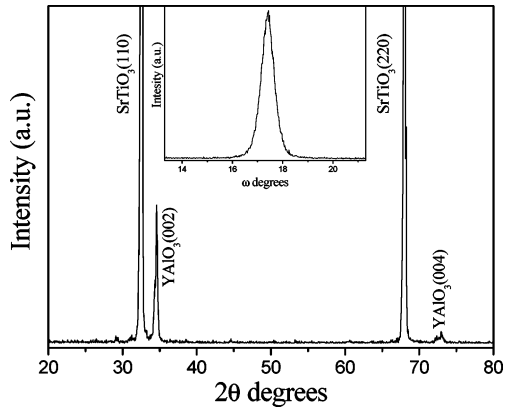

Figure 2. $\theta-2\theta$ XRD scan of a 2 mol % Er^{3+} doped $YAlO_3$ thin film deposited at 1050 °C on $SrTiO_3$ (110) substrate. The inset shows the rocking curve of the (002) reflection.

that mean grain size increases upon increasing the dopant concentration in the films.

Figure 2 shows the $\theta-2\theta$ X-ray diffraction (XRD) pattern of a film deposited at 1050 °C and doped with Er^{3+} at a concentration of 2 mol %. The two reflections observed at $2\theta = 34.60°$ and 73.00°, in addition to those expected for the (110) and (220) of the $SrTiO_3$ substrate, are associated with the (002) and (004) reflections of the orthorombic $YAlO_3$ perovskite structure. The $\theta-2\theta$ pattern clearly indicates a preferred *c*-axis orientation of $YAlO_3$. The out-of-plane orientation has been investigated by recording the rocking curve of the (002) $YAlO_3$ reflection (inset in Figure 2). The full width at half-maximum (fwhm) of rocking curve, giving the spread of grains alignment with respect to substrate, is about 0.58°. This very low value

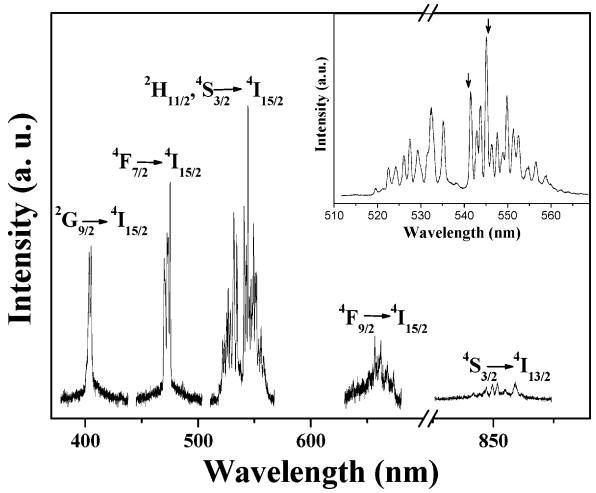

Figure 3. CL spectrum of the $YAlO_3$ film doped with Er^{3+} at a concentration of 2 mol %. The inset shows details of the $^2H_{11/2}$, $^4S_{3/2} \rightarrow {}^4I_{15/2}$ transitions. Arrows in the inset locate the bands selected for PS calibration.

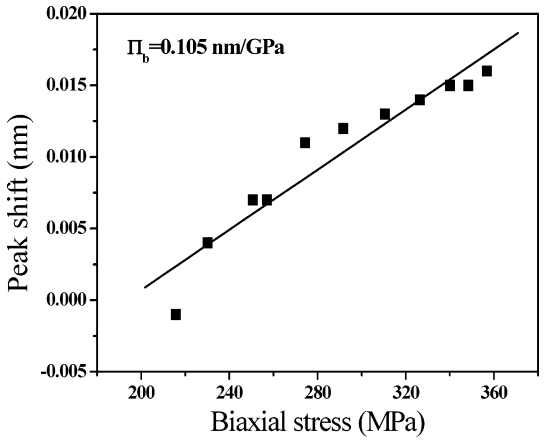

Figure 4. Stress dependence of the 545-nm CL band of Er^{3+} embedded in $YAlO_3$ matrix.

points to a very low grain dispersion of the 2 mol % Er^{3+}:$YAlO_3$ films. Similar results have been found for $YAlO_3$ samples with Er^{3+} concentration of 10 mol %. This suggests that the film grains grew along the *c*-axis, perpendicular to the surface of $SrTiO_3$ substrate with fairly small deviation.

Figure 3 shows the CL spectrum for the $YAlO_3$ thin film doped with 2% mol Er^{3+}. This spectrum was collected at accelerating voltage $V = 10$ kV and beam current $I = 3.14$ nA. CL bands arising from the presence of Er^{3+} dopant can be assigned to the $^2G_{9/2} \rightarrow {}^4I_{15/2}$, $^4F_{7/2} \rightarrow {}^4I_{15/2}$, $^2H_{11/2}$, $^4S_{3/2} \rightarrow {}^4I_{15/2}$, $^4F_{9/2} \rightarrow {}^4I_{15/2}$, $^4S_{3/2} \rightarrow {}^4I_{13/2}$ transitions. These sharp and intense bands are very similar to those observed in the Er^{3+} photoluminescence spectrum, reported elsewhere.[11] No significant changes of shapes and positions of luminescence bands were observed for the 10% mol Er^{3+} doped sample, apart from a decrease of the observed CL intensity value. Spectral positions of the observed transitions in all samples are in agreement with data reported for Er^{3+} ion in bulk $YAlO_3$ single crystals.[40−42]

Because of their higher intensities and better spectral resolution, two different CL bands, related to transitions from the $^4S_{3/2}$ excited state, have been monitored for residual stress assessments in the thin film (cf. inset in Figure 3). Figure 4 shows the stress dependence of the band located at 545 nm for the sample doped with 2% mol Er^{3+}, clearly indicating a spectral shift of the luminescence band ($\Delta\lambda$). However, the spectroscopic shift of luminescence bands usually varies, to a certain degree

TABLE 1: Experimental Results of Stress Dependence for the Two Selected CL Bands of 2 mol % Er^{3+} Doped $YAlO_3$ Films

band (nm)	Π_b (nm Gpa^{-1})	$\pm\Delta\Pi$ (nm GPa^{-1})	R^2
541	0.175	0.034	0.74
545	0.105	0.010	0.90

of precision, linearly with applied stress up to several GPa.[43] The present data appears to deviate from a linear behavior and, strictly speaking, they should be rationalized according to two different slopes, for the high and the low stress ranges. However, we decided to use a single slope for the plot, according to the three following considerations: (1) according to theoretical considerations, the applied stress field is too low to justify a nonlinear piezo-spectroscopic behavior for the CL bands; (2) the error in using a single slope is indeed quite small as compared to the overall average residual stress stored in the film; and (3) the observed nonlinearity of the plot may be related to data scattering arising from residual stress fluctuations because of processing and microstructural mismatch.

Data of stress calibration indicate that the peak shifts toward higher wavelengths upon increasing the applied (tensile) stress. The slope of a linear least-squares fit represents the biaxial PS coefficient, Π_{bi}, and it refers to the modification of electronic energy levels upon stress application. Table 1 summarizes the results of PS calibrations with respect to the selected luminescence peaks. The values of PS coefficients determined for the selected luminescence bands are very similar to those reported for Sm^{3+} doped fluorophosphate and borosilicate glasses[31] and confirm that, in addition to their relative high luminescence efficiency, bands arising from rare-earth activated phosphors can be highly sensitive to stress. Given the relatively smaller scattering of data associated with the peak at 545 nm, we selected this peak for the assessment of residual stresses as described hereafter.

Figure 5A shows a residual stress map ($12 \times 12\ \mu$m) collected on the 2 mol % Er^{3+} doped $YAlO_3$ film. CL spectra were collected at accelerating voltage $V = 10$ kV and beam current $I = 3.14$ nA. These electron impingement conditions correspond to a beam depth of ≈800 nm, as calculated according to the Kanaya−Okayama equation.[44] When comparing the beam depth with the film thickness ($t \approx 400$ nm), it can be considered that the measured stress magnitude corresponds to an average bulk residual stress stored within the Er^{3+}:$YAlO_3$ film. The laterally resolved stress map clearly indicates that the residual stress experienced by the film is always compressive in nature and that the stress distribution remains highly homogeneous over the entire investigated region. The maximum compressive stress value lies in the GPa order and its average value is estimated to be about 1 GPa.

As previously mentioned, residual stresses in thin films are associated with both growth process and thermal expansion mismatch. Stresses lie in the film plane parallel to the film/substrate interface. Thermal stress, because of a mismatch in thermal expansion coefficient between the film and the substrate, is given by the following expression:

$$\sigma = \frac{E_f}{1 - \nu_f} \times (\alpha_f - \alpha_s) \times \Delta T \qquad (6)$$

where E_f and ν_f are the Young's modulus and the Poisson's ratio of the film, respectively, α_f and α_s are the thermal expansion coefficients of film and substrate, respectively, and ΔT is the temperature difference between deposition and room temperatures ($\Delta T = 1025$ K). Since the thermal expansion

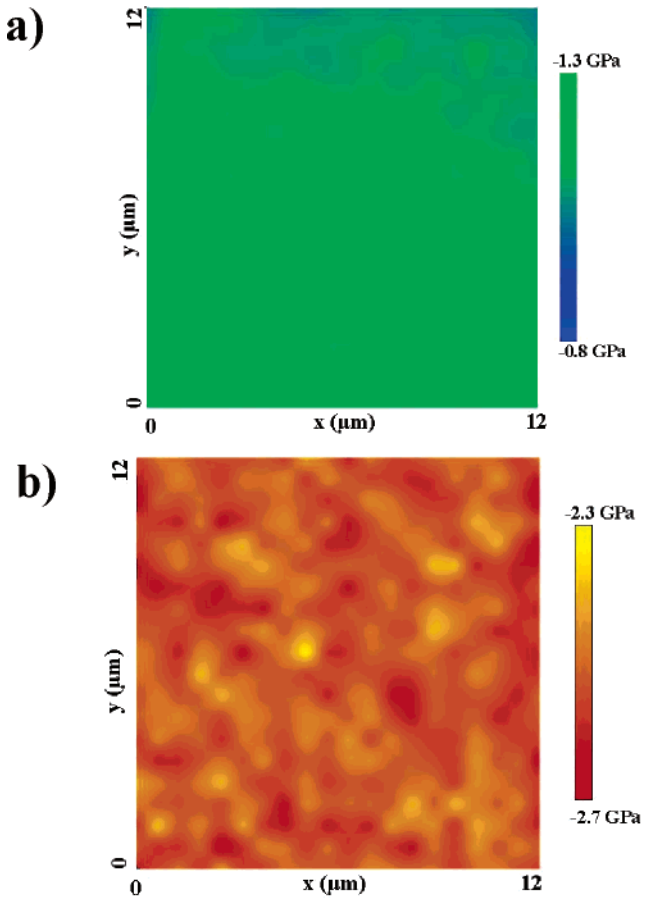

Figure 5. Residual stress distribution in $YAlO_3$ thin film doped with Er^{3+} at a concentration of 2 mol % (a) and 10 mol % (b).

coefficient of the present film ($8.2 \cdot 10^{-6}\ K^{-1}$) is lower than that of the substrate ($10.3 \cdot 10^{-6}\ K^{-1}$), it can be expected that the film undergoes an in-plane compressive stress field upon cooling. Assuming Young's modulus and Poisson ratio of 310 GPa and 0.3, respectively, eq 6 predicts a compressive stress of about 0.9 GPa in the film, which is slightly lower than the average value experimentally determined by CLPS assessment. The overall residual compressive stress in Er^{3+} doped $YAlO_3$ thin films deposited on (110) $SrTiO_3$ substrate is likely due to various factors such as (1) the difference in thermal expansion coefficients between the film and the substrate, (2) the lattice mismatch between film and substrate, and (3) the dopant effect. The good matching between experimental and calculated residual stress values suggests that the thermal expansion mismatch between film and substrate plays a major role in the development of internal stress in the low-doped system.

Figure 5b displays a stress map collected on the 10 mol % Er^{3+} doped $YAlO_3$ film. There is evidence that the residual stress still remains compressive and is uniformly distributed over the entire investigated surface, in analogy with the 2 mol % Er^{3+} doped $YAlO_3$ film. Nevertheless, the compressive residual stress increases upon increasing dopant concentration, varying in the interval between 2.3 and 2.7 GPa for the 10 mol % doped sample. Since both the present films have been deposited under the same experimental conditions, the observed variations of the residual stress can be associated with an intrinsic effect associated with the dopant concentration.

Conclusion

In the present study, we have investigated the residual stress field developed in Er^{3+} doped $YAlO_3$ thin films deposited on

(110) $SrTiO_3$ substrates by the MOCVD approach. $\theta-2\theta$ scans and rocking curves revealed the formation of a pure orthorhombic $YAlO_3$ phase, having (001) orientation and superior out-of-plane alignment. Quantitative information on the magnitude of the residual stress field has been obtained using a PS approach on the basis of the CL spectrum of the trivalent erbium ion. Two different luminescence peaks have been selected and used to determine the relevant correlation between stress and wavelength shifts. Er^{3+} doped $YAlO_3$ thin films deposited on $SrTiO_3$ substrates suffered compressive residual stress, and the average stress value found in both samples was of a GPa order. In addition, the reported data suggest that the residual stress stored in present films strongly depends on dopant concentration. The present study also highlights the suitability of CL spectroscopy for obtaining precise residual stress information on the nanometer scale in thin films.

Acknowledgment. This work has been partially supported by MIUR (Ministero dell'Istruzione, dell'Università e della Ricerca). The authors are grateful to INSTM for providing financial support to R.G.T. for her stay at RIN, Kyoto Institute of Technology.

References and Notes

(1) Buchal, C.; Siegrist, T.; Jacobson, D. C.; Poate, J. M. *Appl. Phys. Lett.* **1996**, *68*, 438.
(2) Capobianco, J. A.; Vetrone, F.; Boyer, J.-C.; Speghini, A.; Bettinelli, M. *J. Phys. Chem. B* **2002**, *106*, 1181.
(3) Heer, S.; Lehmann, O.; Haase, M.; Gudel, H.-U. *Angew. Chem.* **2003**, *42*, 3179.
(4) Hreniak, D.; Strek, W. *J. Alloys Compd.* **2002**, *341*, 183.
(5) Feldmann, C.; Jûstel, T.; Ronda C. R.; Schmidt, P. J. *Adv. Funct. Mater.* **2003**, *13*, 511.
(6) Ryabova, L. A. *Curr. Top. Mater. Sci.* **1981**, *7*, 587.
(7) Sonsky, J.; Lancok, J.; Jelinek, M.; Oswald, J.; Studnicka, V. *Appl. Phys. A: Mater. Sci. Process.* **1998**, *A66*, 583.
(8) Lancok, J.; Jelinek, M.; Grivas, C.; Flory, F.; Lebrasseur, E.; Garapon, C. *Thin Solid Films* **1999**, *346*, 284.
(9) *Chemical Vapor Deposition: Principles and Applications;* Hitchman, M. L., Jensen, K. F., Eds; Academic Press: London, 1993.
(10) Han, B.; Neumayer, D. A.; Schulz, D. L.; Hinds, B. J.; Marks, T. J. *Chem. Mater.* **1993**, *5*, 14.
(11) (a) Malandrino, G.; Grigoli, G.; Fragalà, I. L. *Chem. Mater.*, submitted for publication. (b) Malandrino, G.; Agosta E.; Fragalà, I. L.; Bettinelli, M.; Speghini, A. work in progress.
(12) *Handbook of Nanotechnology*; Bhushan, Ed.; Spinger-Verlag: Berlin, 2004.
(13) Valim, D.; Souza Filho, A. G.; Freire, P. T. C.; Mendes Filho, J.; Guarany, C. A.; Reis, R. N.; Araujo, E. B. *J. Phys. D: Appl. Phys.* **2004**, *37*, 744.
(14) Hovis, D. B.; Hever, A. H. *Scr. Mater.* **2005**, *53*, 347.
(15) Windischmann, H.; Epps, G. F.; Cong, Y.; Collins, R. W. *J. Appl. Phys.* **1991**, *69*, 2231.
(16) Petrov, I.; Losbichler, P.; Bergstrom, D.; Greene, J. E.; Munz, W.-D.; Hurkmans, T.; Trinh, T. *Thin Solid Films* **1997**, *302*, 179.
(17) Fu, D. S.; Iwazaki, H.; Suzuki, H.; Ishikawa, K. *J. Phys.: Condens. Matter* **2000**, *12*, 399.
(18) Ma, W.; Zhang, M.; Yu, T.; Chen, Y.; Ming, N. *Appl. Phys. A: Mater. Sci. Process.* **1998**, *60A*, 345.
(19) Sun, L.; Chen, Y. F.; He, L.; Ge, C. Z.; Ding, D. S.; Yu, T.; Zhang, M. S.; Ming, M. B. *Phys. Rev. B* **1997**, *55*, 12218.
(20) Fu, D.; Ogawa, T.; Suzuki, H.; Ishikawa, K. *Appl. Phys. Lett.* **2000**, *77*, 1532.
(21) Lee, C. J.; Pezzotti, G.; Okui, Y.; Nishino, S. *Appl. Surf. Sci.* **2004**, *228*, 10.
(22) Popovici, G.; Xu, G. Y.; Botchkarev, A.; Kim, W.; Tang, H.; Salvador, A.; Morkoc, H.; Strange, R.; White, J. O. *J. Appl. Phys.* **1997**, *82*, 4020.
(23) Ma Q.; Clarke, D. R. *J. Am. Ceram. Soc.* **1993**, *76*, 1433.
(24) Pezzotti, G. *J. Raman Spectrosc.* **1999**, *30*, 867.
(25) Ohno, T.; Fu, D.; Suzuki, H.; Miyazaki, H.; Ishikawa, K. *J. Eur. Ceram. Soc.* **2004**, *24*, 1669.
(26) Laukaitis, G.; Lindroos, S.; Tamulevicius, S.; Leskela, M.; Rackaitis, M. *Mater. Sci. Eng. A* **2000**, *288*, 223.
(27) Binning, G.; Quate, C. F.; Gerber, G. *Phys. Rev. Lett.* **1986**, *56*, 930.
(28) Cardinale, G. F.; Howitt, D. G.; McCarty, K. F.; Medlin, D. L.; Mirkarimi, P. B.; Moody, N. R. *Diamond Relat. Mater.* **1996**, *5*, 1295.
(29) Saha, R.; Nix, W. D. *Acta Mater.* **2002**, *50*, 23.
(30) Ostertag, C. P.; −Krasicka, E. D. *J. Mater. Sci.* **1999**, *34*, 557.
(31) Pezzotti, G. *Microsc. Anal.* **2003**, *33*, 5.
(32) Pezzotti, G.; Leto, A.; Tanaka, K.; Sbaizero, O. *J. Phys.: Condens. Matter* **2003**, *15*, 7687.
(33) Leto, A.; Pezzotti, G. *J. Phys.: Condens. Matter* **2004**, *16*, 4907.
(34) Malandrino, G.; Lo Nigro, R.; Fragalà, I. L.; Benelli, C. *Eur. J. Inorg. Chem.* **2004**, *3*, 500.
(35) McAleese, J.; Plakatouras, J. C.; Steele, B. C. H. *Thin Solid Films* **1996**, *280*, 152.
(36) Wan, K.; Zhu, W.; Pezzotti, G. *Meas. Sci. Technol.* **2006**, *17*, 181.
(37) Vitman, F. F.; Pukh, V. P. *Zavod. Lab.* **1963**, *92*, 863.
(38) Hertz, H.; Reiner, J. *Angew. Math.* **1882**, *92*, 156.
(39) Grabner, L. *J. Appl. Phys.* **1978**, *49*, 580.
(40) Kaminskii, A. A. *Laser Crystals, Their Physics and Properties*; Springer: Berlin, 1981.
(41) O'Hare, J. M.; Donlan, V. L. *Phys. Rev. B* **1977**, *15*, 10.
(42) Francini, R.; Pietrantoni, S.; Zimbelli, M.; Speghini, A.; Bettinelli, M. *J. Alloys Compd.* **2004**, *380*, 34.
(43) Forman, R. A.; Piermarini, G. J.; Barnett, J. D.; Block, S. *Science* **1972**, 176, 284.
(44) Kanaya, K.; Okayama, S. *J. Phys. (Paris) D: Appl. Phys.* **1972**, *5*, 43.